



## Journal of Advanced Research in Applied Mechanics

Journal homepage:  
[https://semarakilmu.com.my/journals/index.php/appl\\_mech/index](https://semarakilmu.com.my/journals/index.php/appl_mech/index)  
ISSN: 2289-7895



# Analysis on the Effect of Elevated Loading of Reclaimed Spent Bleach Earth on Physico-Mechanical Properties of PLA Polymer Composite in Single Screw Extrusion Process

Zurina Shamsudin<sup>1,\*</sup>, Adibah Haneem Mohamad Dom<sup>1</sup>, Muhammad Afiq A. Razak<sup>1</sup>, Masturah Mesri<sup>2</sup>, Mulyadi<sup>3</sup>

<sup>1</sup> Faculty of Manufacturing Engineering, Universiti Teknikal Malaysia Melaka, Hang Tuah Jaya, 76100 Durian Tunggal, Melaka, Malaysia

<sup>2</sup> Research Institute and Commercialization (RIC), Universiti Teknologi Petronas, 32610 Seri Iskandar, Perak Darul Ridzuan, Malaysia

<sup>3</sup> Institut Teknologi Medan, Kota Medan, 20217 Sumatera Utara, Indonesia

### ARTICLE INFO

#### Article history:

Received 25 August 2023

Received in revised form 27 October 2023

Accepted 13 November 2023

Available online 5 January 2024

#### Keywords:

PLA composite; reclaimed spent bleach earth; extrusion process; physico-mechanical properties

### ABSTRACT

Wood has found widespread use in various applications, however, this extensive usage has resulted in adverse environmental effects, such as contributing to global warming. To mitigate these impacts, there is potential in utilizing reclaimed spent bleach earth (SBE) as an alternative source for biocomposite materials. While polylactic (PLA) polymer is biodegradable, it exhibits limited mechanical properties. This study aims to explore the feasibility of incorporating SBE into polymer matrices. Different filler loading percentages for the PLA/SBE composite (0 wt.%, 10 wt.%, 20 wt.%, 30 wt.%, and 40 wt.%) and extruder temperatures (170°C and 180°C) were considered. The SBE powder underwent characterization using techniques including Particle Size Analysis (PSA), X-Ray Diffraction (XRD), and Field Emission with Energy Dispersive X-Ray (FESEM-EDX). Characterization data revealed that SBE particles ranged in size from 40.24  $\mu\text{m}$  to 51.37  $\mu\text{m}$  and exhibited a crystalline structure. Density of the SBE/PLA composite directly correlated with composition, whereas tensile strength and Young's modulus displayed an inverse relationship. Moreover, varying the temperature by 10°C did not result in significant property changes. The connection between properties and SBE filler loading was evident through alterations in density and Young's modulus values. Furthermore, the composite's behavior shifted from ductile to brittle. Examination of surface fractures through fractography established a link between composite properties, filler loading, and temperature. Images of all samples displayed well-dispersed structures without significant voids. In conclusion, ANOVA analysis indicated that filler loading significantly impacted strength properties. These findings serve as a valuable addition to the existing database, which is currently limited in its coverage of SBE/PLA polymer composites, particularly in applications like packaging.

\* Corresponding author

E-mail address: [zurina.shamsudin@utem.edu.my](mailto:zurina.shamsudin@utem.edu.my)

<https://doi.org/10.37934/aram.112.1.162174>

## 1. Introduction

Wood is a commonly used material in packaging. Examples of wooden packaging materials include pallets, boxes, and other containers made from wood. Utilizing wood as a source for green packaging is environmentally friendly due to its complete biodegradability and recyclability. However, the use of wood can have negative environmental consequences, such as contributing to deforestation and global warming.

To mitigate the impact of increased wood consumption on global warming, reclaimed spent bleach earth (rSBE) is being considered as a potential substitute for wood in packaging materials [1-3]. SBE, typically treated as waste requiring landfill disposal, possesses untapped useful resources that can find applications in various industries and the environment. While previous research has primarily focused on SBE regeneration and other applications like fuel source, biodiesel, and non-fired wall tiles, its potential in polymer composites has been relatively underexplored [4-10]. Natural sources, such as waste agriculture, are susceptible to insect damage and exhibit limited mechanical properties, affecting aspects like moisture resistance, warping, and strength properties. To address this, incorporating SBE, which has limited mechanical properties, into polymer composites can enhance their strength attributes.

Poly(lactic acid) (PLA) polymer, although biodegradable and insect-resistant, suffers from inherent low mechanical properties, including brittleness, low heat distortion temperature, and slow crystallization rate as stated by Su *et al.*, [11]. The incorporation of SBE as a cost-effective reinforcement in biocomposites offers a sustainable approach to enhancing PLA's mechanical properties and maximizing SBE utilization. In the fabrication of biocomposites, filler loading is a key determinant of composite performance. Melt processing parameters such as temperature and screw speed play crucial roles, affecting mechanical properties and final composite characteristics [12]. Thus, this study aims to enlighten the use of SBE in biocomposites, focusing on the percentage loading for the composite and extruder temperature.

The introduction of SBE/PLA as an alternative biocomposite in packaging materials holds promise for practical industrial applications, considering future perspectives and concerns.

## 2. Methodology

As part of the preliminary steps in obtaining reclaimed SBE, the material underwent cleaning and drying procedures. The SBE waste was sourced from Mewah Oil Sdn Bhd in Port Klang, an industry contributor. The extraction process was then employed to extract oil from the SBE, using Hexane as the chemical solvent.

The SBE powder was mixed with Hexane in a beaker and subjected to ultrasonic treatment in an ultrasonic machine for five cycles of half an hour each. The oil was removed during the intervals and subsequently dried at room temperature before sieved using size mesh 75 $\mu$ m. The particle sizes of the reclaimed SBE (rSBE) were determined through particle size analysis using the Mastersizer 2000 (Malvern Instrument Ltd model).

The poly(lactic acid) (PLA) used in this study was initially in pellet form and underwent drying in a Memmert oven at 80°C for three hours. This ensured the complete absence of moisture in the PLA prior to the mixing process via the ball mill technique. The composition weight percentages for reclaimed SBE included 0 wt.%, 10 wt.%, 20 wt.%, 30 wt.%, and 40 wt.%, summing up to 100 wt.% of PLA polymer, as depicted in Table 1. Table 2 presented the parameter processing of single screw extruder for mixing process.

To analyze physical properties, bulk density was assessed following ASTM D693 procedure. Microstructures were observed using Field Emission Dispersive X-Ray (FESEM)-EDX at an accelerated 10 kV, with gold layers applied to the sample surfaces to ensure conductivity using the SC-7620 mini sputter. The phases of rSBE sample were analyzed using X-ray diffraction (XRD), and strength properties were evaluated through Ultimate Tensile Machine (UTM) testing according to ASTM D3039. Lastly, ANOVA analysis using two level factorial was applied to interpret the factors influencing strength properties.

**Table 1**  
 Composition preparation of PLA and reclaimed spent bleach earth composite

Code	Composition (wt.%)	
	PLA	rSBE
SBE 0	100	0
SBE 10	90	10
SBE 20	80	20
SBE 30	70	30
SBE 40	60	40

**Table 2**  
 Parameter processing of single screw extruder machine

No.	Parameter Processing		
	Speed (rpm)	Temperature (°C)	Batch
1.	35	170	rSBE0, rSBE10, rSBE20, rSBE30, rSBE40
2.	35	180	rSBE0, rSBE10, rSBE20, rSBE30, rSBE40

### 3. Results

#### 3.1 Particle Size of SBE Distribution Analysis

The frequency distribution analysis of particle size provides insights into the quantity of particles existing within specific size intervals. In particle-reinforced polymer composites, particle size information is a crucial factor that influences the entire processing journey toward achieving desired final product properties. The mechanical attributes of particulate-polymer composites are significantly impacted by particle size, particle-matrix interface adhesion, and particle loading. These mechanical properties are notably affected by particle size, as indicated by Xu *et al.*, in 2018 [13], suggesting the potential for enhanced mechanical characteristics. The influence of particle size extends to the mixing process within the extrusion mechanism.

Figure 1 illustrates the particle size distribution of reclaimed spent bleach earth (rSBE). The results indicate a particle size range from 0.634  $\mu\text{m}$  to 174.1  $\mu\text{m}$ , with a predominant particle size falling between 40.24  $\mu\text{m}$  and 51.371  $\mu\text{m}$ , constituting 19.28% of the volume. Despite the use of a 75  $\mu\text{m}$  sieve shaker during the sieving process, particles exceeding 75  $\mu\text{m}$  are still present. This could be attributed to the natural characteristics of rSBE, including its sensitivity to humidity and tendency to clump when exposed to the environment before the fabrication process. Consequently, some particles may already be clumped together during particle size analysis.

Even though particles larger than 75  $\mu\text{m}$  are present, the graph demonstrates that 50% of particle sizes are smaller than 35.76  $\mu\text{m}$ , and 90% are smaller than 86.32  $\mu\text{m}$ . While some particles are larger than 75  $\mu\text{m}$ , the difference in size isn't substantial, making their use suitable. In line with research conducted by Qi *et al.*, in 2022 [14], investigations were carried out with particles ranging from 20 to over 120 mesh size. The outcome revealed that particles beyond 120 mesh size exhibited good

homogeneity. Consequently, the sieve-obtained size is viable for use, and smaller particle sizes are preferable as they contribute to greater homogeneity when combined with other materials.

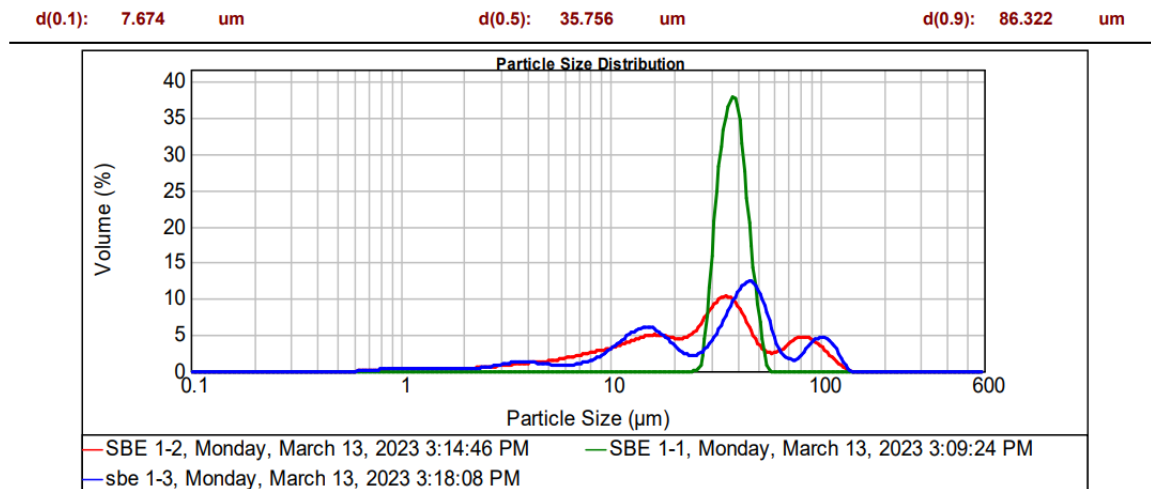
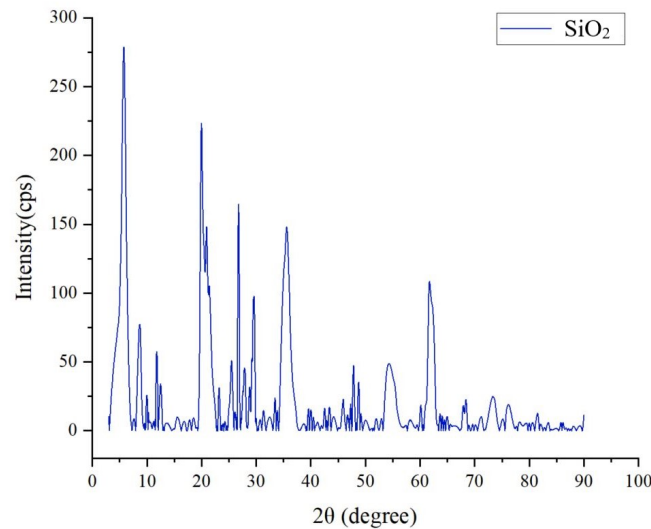


Fig. 1. Particle size of reclaimed spent bleach earth (rSBE)

### 3.2 Phase, Microstructure and Element Analysis

Figure 2 displays the X-ray diffraction (XRD) pattern of the rSBE, revealing its chemical composition. The diffractogram illustrates prominent peaks indicating the presence of various chemical constituents within the rSBE. Notably, silicon dioxide ( $\text{SiO}_2$ ) exhibits the highest peak at  $2\theta = 5^\circ$ , succeeded by calcium oxide ( $\text{CaO}$ ) at  $2\theta = 21^\circ$ , ferric oxide ( $\text{Fe}_2\text{O}_3$ ) at  $2\theta = 35^\circ$ , and aluminum oxide ( $\text{Al}_2\text{O}_3$ ) at  $2\theta = 63^\circ$ . As the SBE originates from palm waste, its chemical composition is diverse, encompassing multiple elements. This aligns with Yusnimar *et al.*, [15] findings, which suggest that SBE belongs to the bentonite or clay category, primarily comprising  $\text{SiO}_2$ ,  $\text{Al}_2\text{O}_3$ ,  $\text{Fe}_2\text{O}_3$ ,  $\text{CaO}$ , and  $\text{MgO}$ . The distinct peaks in the graph correspond to different elements present in the SBE, indicating its multi-elemental and multi-phasic nature. The well-defined peaks further signify that the SBE is in a crystalline phase.

The microstructure and elemental composition of the rSBE were analyzed using field emission scanning electron microscopy coupled with energy-dispersive X-ray spectroscopy (FESEM-EDX), as depicted in Figure 3. This analytical technique enables the identification of chemical composition and the morphology of the raw material. Oxygen constitutes the highest percentage in all elements, followed by silicon and other trace elements. This predominance of oxygen can be attributed to the oxide-based composition of the rSBE, with silicon playing a significant role. Work from Yusminar *et al.*, [15] affirm that SBE, like bentonite, primarily comprises  $\text{SiO}_2$  (silica), which accounts for around 83.5% of its composition. Consequently, the elevated oxygen content reflects the oxide-rich nature of the SBE, with silicon being the subsequent prevalent element.



**Fig. 2.** Phase analysis of spent bleach earth (SBE)

The distinctive angular shape of rSBE is akin to that of angular and crushed glass particles, as evidenced by their granulometric distribution according to Letelier *et al.*, in 2019 [16]. This observation aligns with the XRD results displayed in Figure 2, which correlates the crystalline phase of rSBE with its uneven shape, indicated by sharp intensity peaks.

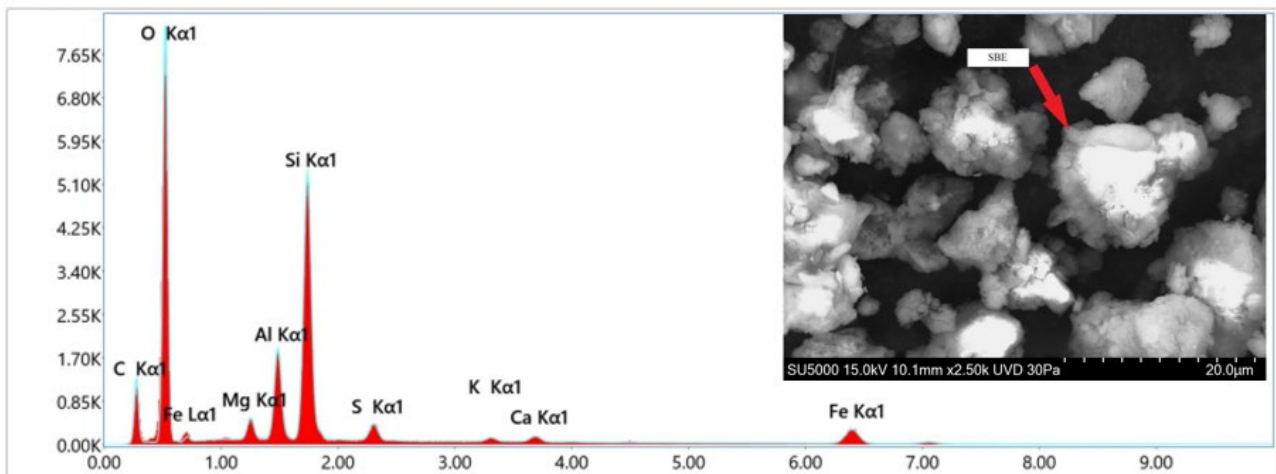


**Fig. 3.** The chemical composition and microstructure of SBE

### 3.3 Physico-Mechanical Properties

Figures 4, 5, and 7 depict densities, tensile strength, and modulus at varying processing temperatures and SBE filler loadings. The figures demonstrate that with increasing SBE loading, physico-mechanical properties exhibit fluctuating patterns at specific processing temperatures. The investigation into the physical properties of composites at different loading and extrusion temperatures involved density testing, while mechanical properties were assessed through tensile testing.

### 3.3.1 Density measurement

Figure 4 depicts the variations in density of PLA/rSBE composites across different SBE filler loadings: 0 wt.%, 10 wt.%, 20 wt.%, 30 wt.%, and 40 wt.%, at varying temperatures. Notably, Figure 4 reveals that the loading remains consistent between 170°C and 180°C, showing a direct proportionality. Although slight variations in density are observed when adding 10% to 40% rSBE at temperatures of 170°C and 180°C, the difference is not substantial. This suggests that a temperature increase of 10°C from 170°C does not significantly impact density enhancement. Low standard deviation values for both temperatures indicate remarkable data consistency. The findings underline that an additional 10°C has negligible influence on the density of the rSBE/PLA composite.

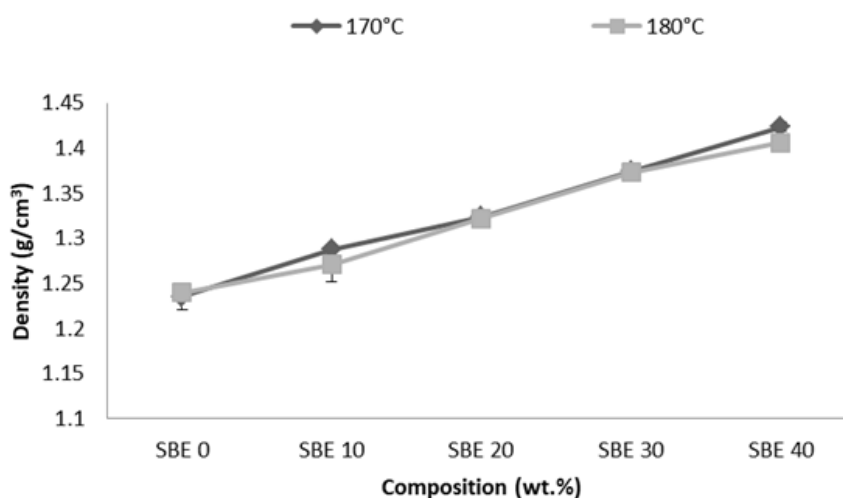


Fig. 4. Density of PLA/rSBE composite at different temperature and filler loading

However, the anticipated inverse relationship between filler loading percentage and density is not evident. Typically, composite creation aims to reduce density, imparting lightweight properties. According to Abid, Vineet, & Lalit [17], PLA possesses a density of 1.25 g/cm<sup>3</sup>, while Kenaf, similar to SBE, has a density of 1.2 g/cm<sup>3</sup> [18]. Following the law of mixture, the density of 40 wt.% SBE should be below 1.2 g/cm<sup>3</sup>. Surprisingly, the result indicates a higher value than both pure PLA and rSBE.

One plausible factor influencing density is water absorption, a characteristic of natural waste materials. Water absorption is influenced by factors like exposed surface area, exposure period, diffusivity, temperature, fiber content, permeability, orientation, and surface protection as reported in [19,20]. The density test, based on the Archimedes principle, requires sample submersion in water to measure the displaced water weight—an approach not ideal for measuring natural fibers. Thus, when testing follows the Archimedes principle and particle size is small, water absorption increases as filler loading rises. This elucidates why pure PLA exhibits the lowest density, while 40 wt.% rSBE demonstrates the highest density due to its significant natural waste content.

### 3.3.2 Ultimate strength analysis

Illustrated in Figure 5 is the ultimate tensile strength of the composite. This figure vividly portrays how an escalation in filler loading proportion leads to a reduction in the tensile strength of the PLA/rSBE composite across both temperatures. This observation underscores the inverse correlation between tensile strength and filler loading, which further varies with temperature shifts. The disparities in tensile strength were not substantial, with an average difference of approximately 10%,

equivalent to 1 to 4 MPa. Similar to the findings of Barczewski's research in 2017[21], the minimal standard deviation signifies minimal error, ensuring consistency across results.

As indicated by Figure 5, the highest tensile strength, 15.12 MPa fits to pure PLA at a temperature of 180°C. Conversely, the lowest value, 3.437 MPa is associated with 40 wt.% rSBE. This observation may be intertwined with the density outcome and microstructure of 40% rSBE (Figure 6), where increased density and water absorption are evident. Consequently, a surge in density correlates with a decrease in tensile strength.

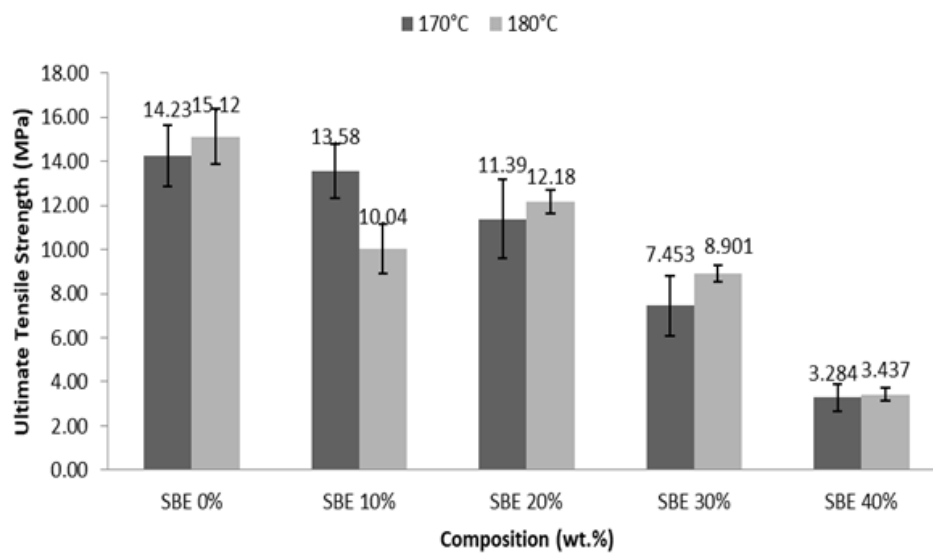


**Fig. 5.** Ultimate tensile strength (UTS) of PLA/rSBE composite at different temperature and various filler loading

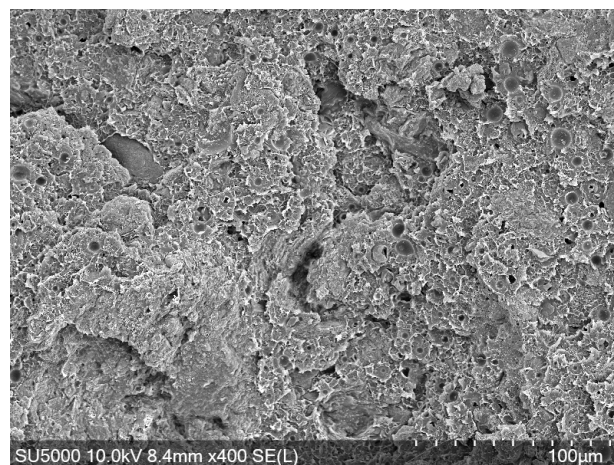


**Fig. 6.** The microstructure of PLA/rSBE composite of 40 wt.% rSBE

### 3.3.3 Modulus analysis

Depicted in Figure 7 is the Young modulus across two distinct temperatures, highlighting the interaction between temperature and filler loading on Young modulus. As illustrated, the Young modulus of the PLA/rSBE composite experiences a decline with an increase in both filler loading and temperature. This trend points out the inverse relationship between Young modulus and both filler loading and temperature. Notably, the highest Young modulus of pure PLA occurs at a temperature

of 170°C, measuring 1.339 GPa, while the lowest value of 0.356 GPa is observed at 40 wt.% rSBE. The Young modulus and tensile strength exhibit parallel trends, inversely proportional to temperature and filler loading. This can be seen from the relationship between stress and strain, with stress being directly linked to breaking force. Consequently, as force diminishes, stress follows suit.

The outcomes of the tensile test reveal that an increase in filler loading correlates with decreased force and stress values. However, previous research integrating PLA with natural resources suggests that composite mechanical properties elevate with filler loading until a certain composition, beyond which degradation commences. Ahmad, Hassan, and Chen's study in 2020 [22] provides evidence of this phenomenon, wherein the PLA-Kenaf fiber (KF) composite displays enhanced mechanical properties up to 30 wt.% KF, but at 40 wt.%, properties start declining, indicative of material degradation. This aligns with the concept that particle size impacts properties; although micro-sized, SBE particles do not lead to enhanced tensile strength with increasing filler loading, in contrast to earlier studies.

Furthermore, Qi *et al.*'s research in 2022[14] highlights that while tensile strength improves as mesh size increases from 20 to over 120 mesh size, this trend doesn't hold solid for SBE particles. Despite their small size, rSBE particles do not exhibit improved tensile strength with escalating filler loading, contrary to previous findings.

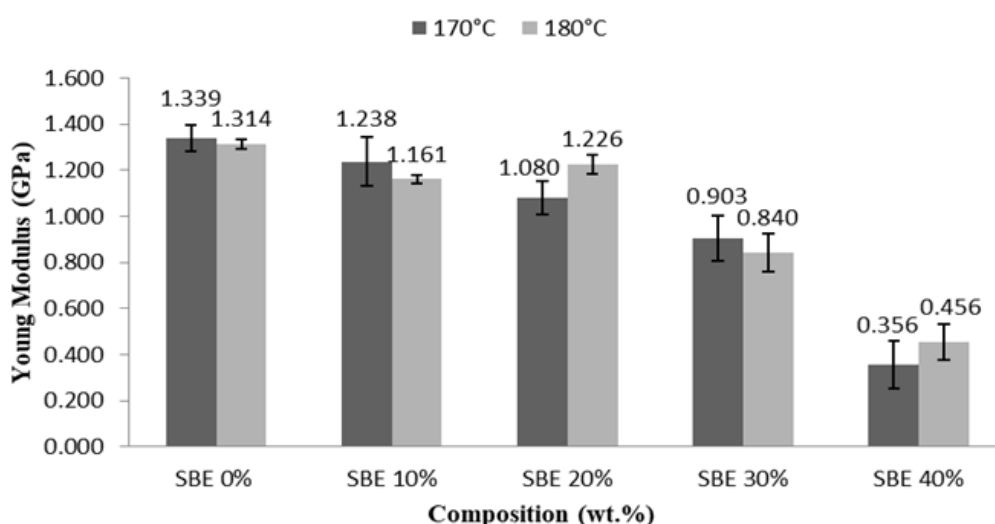


**Fig. 7.** Young modulus of PLA/rSBE composite at different temperature and various filler loading

Figure 8 presents the microstructure of the PLA/rSBE composite, revealing a well-mixed composite where PLA encapsulates rSBE. This encapsulation is evident through the presence of a smoothly fractured surface and the occurrence of small voids. The presence of voids is expected due to particle pull-out post-sample testing. However, despite this microstructure, the mechanical attributes of the composite deteriorate with increasing filler loading, contrary to findings from the previous study [22]. Their research on PLA/Kenaf Fiber composites demonstrated enhanced mechanical properties with increased filler loading. A potential explanation for the contrasting behavior observed in the PLA/rSBE composite could be attributed to poor compatibility between PLA and rSBE. Poor compatibility often leads to diminished mechanical characteristics, as noted by Qi *et al.*, in 2022 [14]. It's important to note that PLA in its pure form possesses limited mechanical properties. Gultom *et al.*'s investigation in 2020 [23] aligns with this, reporting that PLA displays high brittleness, low heat distortion, and slow crystallization rate. Similarly, rSBE, being a natural waste



material in particle form, also exhibits reduced mechanical properties. Combining PLA, which inherently exhibits weaknesses in mechanical properties, with SBE may consequently lead to decreased tensile strength and Young modulus in the composite as filler loading increases.

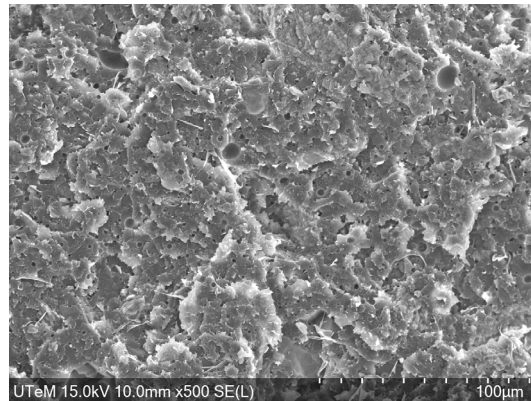


**Fig. 8.** The microstructure of PLA/rSBE composite of 30 wt.% SBE at 170°C

### 3.4 Microstructure Analysis

Microstructure analysis was undertaken to discern the presence of pores within the PLA/rSBE composite, as well as to assess the surface condition of samples in relation to varying filler loadings and processing temperatures. Fractography serves to reveal distinct modes of failure, offering insights into the origin or nature of defects and shedding light on long-term fracture behavior. For the purpose of discussion and attribute identification, two compositions at distinct temperatures were selected. Figure 9 portrays the microstructure of a PLA/rSBE composite with a 10 wt.% loading, while Figure 10 illustrates the microstructure of a PLA/rSBE composite with a 40 wt.% loading.

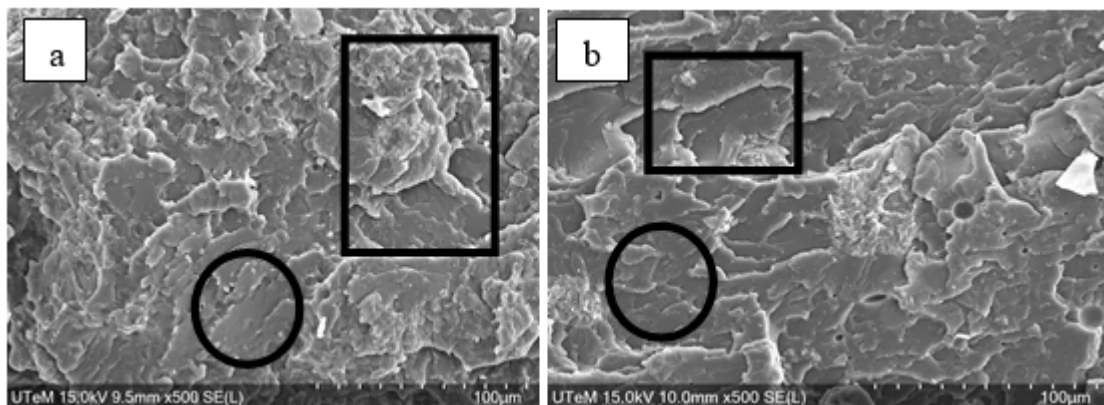


**Fig. 9.** Microstructure of PLA/rSBE composite with (a) 10wt.% rSBE (170°C) (b) 10 wt.% rSBE (180°C)

Analyzing Figure 9 reveals that the microstructure of the composite appears uniformly blended across both temperatures. The absence of pores, voids, or agglomerations within the structure attests to its thorough mixing. A specific circled area in Figure 9 highlights the well-consolidated and dispersed presence of rSBE within the PLA matrix, yielding a smooth surface at the fracture site. However, rSEM images clearly illustrate morphological disparities between 10% and 40%, with a slightly greater homogeneity observed at 180°C compared to 170°C. This suggests that a temperature of 180°C fosters a more homogeneous blend. The squared area emphasized in Figure 9 exhibits a

wave pattern akin to the microstructure of a 10 wt.% PLA/Chestnut shell (CN) composite, as observed by Barczewski in 2017 [21]. This wave pattern is associated with higher tensile strength, indicating the presence of polymer ligaments in the microstructure, rendering the composite more ductile. This connection extends to the tensile strength and Young modulus results, where the 10 wt.% composition outperforms the 40 wt.% counterpart. The presence of polymer bridges lends strength and ductility to the composite, elevating its overall value.

Turning to Figure 10, the microstructure for the 40 wt.% composition demonstrates equally impressive dispersion, characterized by the absence of substantial pores, voids, or agglomerations. rSBE is effectively dispersed and integrated within the PLA matrix, with smooth surfaces evident in the images. Notably, the microstructure is more distinct in Figure 10b than in Figure 10a, indicating a greater homogeneity at 180°C than at 170°C. In contrast to the microstructure in Figure 9, the structure here appears granular, with the wave pattern less pronounced. This distinctive structure signifies a propensity for sudden fracture without significant stretching—a feature of brittle behavior. This brittle behavior and microstructure mirror the findings in previous study [22] on PLA/CN composite. Consequently, the tensile strength and Young modulus of this structure lag behind those of the other composition. While the PLA and rSBE blend well, their mechanical properties are insufficient to withstand high forces, resulting in the observed brittle behavior.

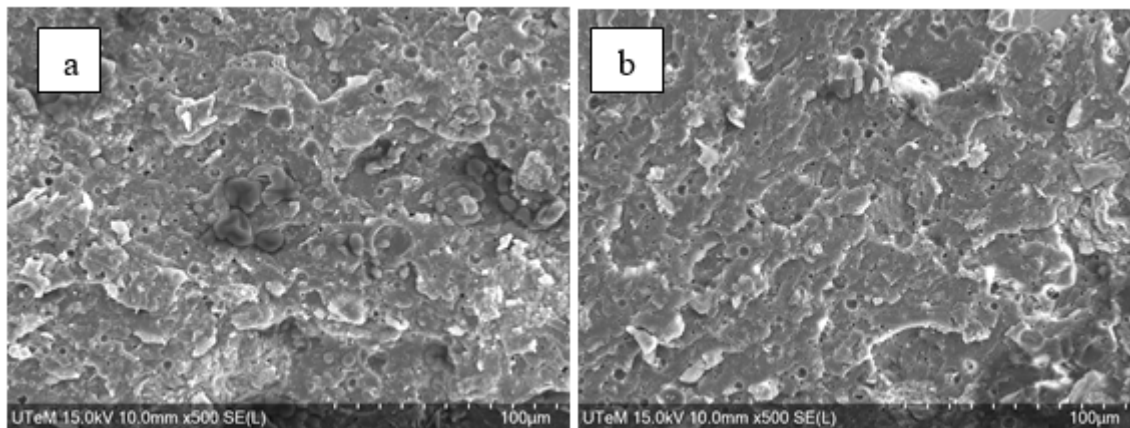


**Fig. 10.** Microstructure of PLA/rSBE composite: (a) 40wt.%rSBE (170°C) (b) 40 wt.% rSBE (180°C)

### 3.5 ANOVA Analysis

Table 3 presents the p-values for all outcomes and factors, serving as a crucial indicator in the ANOVA analysis. In this context, the p-value serves the purpose of evaluating the validity of the model and the influence of factors on the experiment's results. A p-value less than 0.05 indicates the model's significance and the factors' impact on the experiment. Conversely, a p-value exceeding 0.05 implies a lack of significance, rendering the factor's influence negligible or non-existent. It is also evident that the p-value for the model stands at 0.0001, which falls below the 0.05 threshold, validating the model's significance and appropriateness for application. Among the two factors and three outcomes analyzed, only factor B, representing filler loading, exhibits a p-value less than 0.05 across all three outcomes. In contrast, the remaining factors display p-values exceeding 0.05. This implies that factor B, or filler loading, significantly impacts the enhancement of composite strength properties.

However, it's important that the research also discovers an interesting observation. Specifically, as the filler loading fraction increases, the strength properties of the composites actually decline. This behavior arises due to the intricate interplay of material characteristics and the experimental procedures employed as stated in [24]. While ANOVA analysis suggests that filler loading may

influence composite strength properties, it's important to acknowledge that additional variables, including material properties and potential sources of error such as human factors, could also contribute to the outcomes of the strength properties.

**Table 3**

The summary of the analysis based on the factors and responses

Item	Intercept	A (Temperature)	B (Loading)	AB
Density	1.32538	-0.00334	0.0898	-0.00272
p-value		0.1196	< 0.0001	0.3364
Tensile Strength	9.9614	-0.0254	- 5.2521	0.3503
p-value		0.9671	0.0007	0.6892
Young Modulus	0.99535	0.00407	- 0.43791	0.03027
p-value		0.9391	0.0009	0.6899

In Figure 11, an intriguing correlation emerges between young modulus and tensile strength, as evidenced by the proportional and harmonious alignment of regression lines. This observation resonates with findings from the research conducted by Penjumras *et al.*, [25]. The congruence in these regression lines signifies the critical role of filler loading in the experiment, exerting a substantial influence on its outcomes. This influence becomes evident when examining the alterations in physio-mechanical properties resulting from the introduction of filler loading. Importantly, the minor temperature difference of 10°C fails to induce significant property changes. However, it's worth noting that deviations beyond 10°C could potentially yield different outcomes in ANOVA analyses.

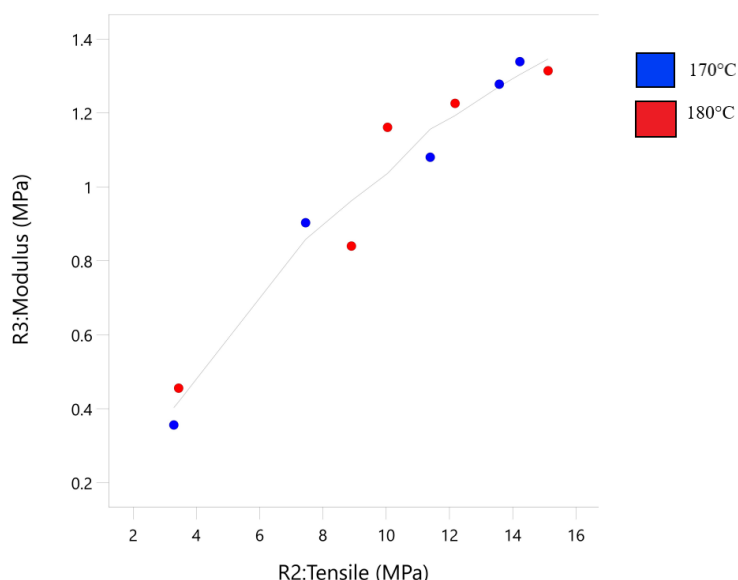


**Fig. 11.** Scatterplot for temperature

#### 4. Conclusions

The testing phase was executed successfully, encompassing SBE characterization and assessments of both physical and mechanical properties. Notably, an increase in filler loading percentage yielded notable shifts in physio-mechanical attributes. Specifically, density exhibited a direct proportionality to filler loading, while both tensile strength and Young modulus displayed an inversely proportional relationship with the filler loading. Intriguingly, variations of 10°C in the extrusion process temperature failed to induce significant alterations in the physio-mechanical

properties. Several factors contributed to these observations, including particle size, filler loading, and material properties. The microstructural examination unveiled distinct behavioral trends, wherein lower filler loading compositions exhibited ductile behavior capable of withstanding considerable force. On the other hand, higher compositions rendered the composite more brittle compared to pure PLA. Although the composite manifested a homogeneous blend, the properties did not surpass those of pure PLA. These discoveries underscore the need for further exploration into the mechanical properties of PLA composites reinforced with natural sources. Additionally, a call is made for the establishment of standardized parameters for processing such composites. This avenue of investigation holds the potential to yield valuable insights and advancements in the realm of sustainable material development.

### Acknowledgement

The authors would like to acknowledge the support by Centre for Research and Innovation Management, Universiti Teknikal Malaysia, Melaka and research team from Research Institute and Commercialization (RIC), Universiti Teknologi Petronas. This research was not funded by any grant.

### References

- [1] Musa, Mohd Lukman, Ramli Mat, and Tuan Amran Tuan Abdullah. "Optimised biofuel production via catalytic cracking of residual palm oil recovered from spent bleaching earth (SBE) over Ni/HZSM-5 Zeolite." *Journal of Advanced Research in Fluid Mechanics and Thermal Sciences* 51, no. 2 (2018): 108-123. <https://doi.org/10.9767/bcrec.13.3.1929.456-465>
- [2] Low, Aaron, Rashid Shamsuddin, and Ahmer Ali Siyal. "Economic analysis of waste minimisation and energy recovery from spent bleaching earth." *Cleaner Engineering and Technology* 7 (2022): 100418. <https://doi.org/10.1016/j.clet.2022.100418>
- [3] Abdelbasir, Sabah M., Ahmed I. Shehab, and MA Abdel Khalek. "Spent bleaching earth; recycling and utilization techniques: A review." *Resources, Conservation & Recycling Advances* (2022): 200124. <https://doi.org/10.1016/j.rcradv.2022.200124>
- [4] Suhartini, Sri, Nur Hidayat, and Sieni Wijaya. "Physical properties characterization of fuel briquette made from spent bleaching earth." *biomass and bioenergy* 35, no. 10 (2011): 4209-4214. <https://doi.org/10.1016/j.biombioe.2011.07.002>
- [5] Foo, N. S., S. K. Loh, K. Ismail, and R. T. Bachmann. "Nutrient recovery from anaerobic palm oil mill effluent with thermally regenerated spent bleaching earth using response surface methodology." *Journal of Oil Palm Research* 32, no. 2 (2020): 245-257.
- [6] Loh, Soh Kheang, Kah Yein Cheong, and Jumat Salimon. "Surface-active physicochemical characteristics of spent bleaching earth on soil-plant interaction and water-nutrient uptake: A review." *Applied Clay Science* 140 (2017): 59-65. <https://doi.org/10.1016/j.clay.2017.01.024>
- [7] Srisang, Naruebodee, Siriwan Srisang, Pitiwat Wongpithawat, Korawit The-Eye, Kittipong Wongkeaw, and Chakkarin Sinthoo. "Production of biomass briquette from residual bleaching earth and empty palm bunch." *Energy Procedia* 138 (2017): 1079-1084. <https://doi.org/10.1016/j.egypro.2017.10.119>
- [8] Naser, Jamil, Onoriode P. Avbenake, Fadimatu N. Dabai, and Baba Y. Jibril. "Regeneration of spent bleaching earth and conversion of recovered oil to biodiesel." *Waste Management* 126 (2021): 258-265. <https://doi.org/10.1016/j.wasman.2021.03.024>
- [9] Srisang, Siriwan, and Naruebodee Srisang. "Recycling spent bleaching earth and oil palm ash to tile production: Impact on properties, utilization, and microstructure." *Journal of Cleaner Production* 294 (2021): 126336. <https://doi.org/10.1016/j.jclepro.2021.126336>
- [10] Shamsudin, Zurina, Masturah Mesri, and Rafidah Hassan. "The Effect of Sintering Temperature on Physical Properties of Sintered Green Glass Ceramic Composite (GCC) Using Design of Experiments (DOE) Software." In *International Conference and Exhibition on Sustainable Energy and Advanced Materials*, pp. 175-180. Singapore: Springer Nature Singapore, 2021. [https://doi.org/10.1007/978-981-19-3179-6\\_32](https://doi.org/10.1007/978-981-19-3179-6_32)
- [11] Su, Shen, Rodion Kopitzky, Sengül Tolga, and Stephan Kabasci. "Polylactide (PLA) and its blends with poly (butylene succinate)(PBS): A brief review." *Polymers* 11, no. 7 (2019): 1193. <https://doi.org/10.3390/polym11071193>
- [12] Doagou-Rad, S., Aminul Islam, and Jakob Søndergaard Jensen. "Influence of processing conditions on the mechanical behavior of MWCNT reinforced thermoplastic nanocomposites." *Procedia Cirp* 66 (2017): 131-136.

- <https://doi.org/10.1016/j.procir.2017.03.362>
- [13] Xu, Wenxiang, Yang Wu, and Mingkun Jia. "Elastic dependence of particle-reinforced composites on anisotropic particle geometries and reinforced/weak interphase microstructures at nano-and micro-scales." *Composite Structures* 203 (2018): 124-131. <https://doi.org/10.1016/j.compstruct.2018.07.009>
- [14] Qi, Zhongyu, Baiwang Wang, Ce Sun, Minghui Yang, Xiaojian Chen, Dingyuan Zheng, Wenrui Yao, Yang Chen, Ruixiang Cheng, and Yanhua Zhang. "Comparison of properties of poly (lactic acid) composites prepared from different components of corn straw fiber." *International Journal of Molecular Sciences* 23, no. 12 (2022): 6746. <https://doi.org/10.3390/ijms23126746>
- [15] Yusnimar, Yusnimar, J. N. Rahman, and P. Ningendah. "UTILIZATION SPENT BLEACHING EARTH AS A FILLER OF MATERIAL CONSTRUCTION." *INFO-TEKNIK* 22, no. 1: 13-30. <https://doi.org/10.20527/infotek.v22i1.11209>
- [16] Letelier, Viviana, Bastián I. Henríquez-Jara, Miguel Manosalva, and Giacomo Moriconi. "Combined use of waste concrete and glass as a replacement for mortar raw materials." *Waste Management* 94 (2019): 107-119. <https://doi.org/10.1016/j.wasman.2019.05.041>
- [17] Haleem, Abid, Vineet Kumar, and Lalit Kumar. "Mathematical modelling & pressure drop analysis of fused deposition modelling feed wire." *Int. J. Eng. Technol* 9, no. 4 (2017): 2885-2894. <https://doi.org/10.21817/ijet/2017/v9i4/170904066>
- [18] Kiron, Mazharul Islam. "Kenaf Fiber: Properties, cultivation, production, uses and advantages." *Textile Learner* 10 (2021).
- [19] Ilyas, R. A., M. Y. M. Zuhri, H. A. Aisyah, M. R. M. Asyraf, S. A. Hassan, E. S. Zainudin, S. M. Sapuan et al., "Natural fiber-reinforced polylactic acid, polylactic acid blends and their composites for advanced applications." *Polymers* 14, no. 1 (2022): 202. <https://doi.org/10.3390/polym14010202>
- [20] Mesri, Masturah, Zurina Shamsudin, Rafidah Hasan, and Nurliyana Daud. "Effects of Bentonite and Eggshell as Fillers on Thermal/Physical Properties of Sintered Glass Composite." *Journal of Advanced Research in Fluid Mechanics and Thermal Sciences* 66, no. 2 (2020): 145-157.
- [21] Barczewski, M., D. Matykiewicz, A. Krygier, J. Andrzejewski, and K. Skórczewska. "Characterization of poly (lactic acid) biocomposites filled with chestnut shell waste." *Journal of Material Cycles and Waste Management* 20 (2018): 914-924. <https://doi.org/10.1007/s10163-017-0658-5>
- [22] Hassan, Nur Adilah Abu, Sahrim Ahmad, and Ruey Shan Chen. "Density Measurement, Tensile and Morphology Properties of Polylactic Acid Biocomposites Foam Reinforced with Different Kenaf Filler Loading." *Sains Malays* 49 (2020): 2293-2300. <https://doi.org/10.17576/jsm-2020-4909-26>
- [23] Gultom, Hizkia MV, Tika Paramitha, and Johnner P. Sitompul. "Regeneration of Spent Bleaching Earth for PLA Nanocomposite Filler." In *IOP Conference Series: Materials Science and Engineering*, vol. 1143, no. 1, p. 012061. IOP Publishing, 2021. <https://doi.org/10.1088/1757-899X/1143/1/012061>
- [24] Iliyasu, Ibrahim, James Bitrus Bello, Musa Nicholas Dibal, Ayodeji Nathaniel Oyedeji, Kazeem Adeniyi Salami, and Elijah Oyewusi Oyedeji. "Response surface methodology for the optimization of the effect of fibre parameters on the physical and mechanical properties of deleb palm fibre reinforced epoxy composites." *Scientific African* 16 (2022): e01269. <https://doi.org/10.1016/j.sciaf.2022.e01269>
- [25] Penjumras, Patpen, Russly Abdul Rahman, Rosnita A. Talib, and Khalina Abdan. "Response surface methodology for the optimization of preparation of biocomposites based on poly (lactic acid) and durian peel cellulose." *The Scientific World Journal* 2015 (2015). <https://doi.org/10.1155/2015/293609>